Quest for vortices in photon condensates

Himadri S. Dhar [1,2,*], Zai Zuo [1], João D. Rodrigues,[1] Robert A. Nyman [1], and Florian Mintert[1]

[1]*Physics Department, Blackett Laboratory, Imperial College London, Prince Consort Road, SW7 2AZ, United Kingdom*
[2]*Department of Physics, Indian Institute of Technology Bombay, Powai, Mumbai 400076, India*

We predict that a photon condensate inside a dye-filled microcavity forms long-lived spatial structures that resemble vortices when incoherently excited by a focused pump orbiting around the cavity axis. The finely structured density of the condensates have a discrete rotational symmetry that is controlled by the orbital frequency of the pump spot and is phase coherent over its full spatial extent, despite the absence of any effective photon-photon interactions.

Introduction. Vortices are a ubiquitous phenomenon occurring in a broad range of many-body systems, wherein a robust topological defect prevents a phase singularity at the middle of a circulating pattern. They appear in fluid turbulence [1], magnetic structures in thin films [2], superconductors [3], and atomic condensates [4]. Formation of vortices in a Bose-Einstein condensate (BEC) is ultimately related to superfluidity [5,6], which is a hallmark of phase coherence in quantum systems that arises from interactions between the particles. While quantum coherence is an integral part of conservative quantum systems, the existence of superfluidity and vortices in driven-dissipative systems such as polariton condensates [7,8] is remarkable. It demonstrates that long-range coherence persists beyond typical loss time scales of the system due to the macroscopic nature of condensation [9]. Vortices in BECs may be generated either by flowing the fluid past a static obstacle [8], colliding two condensates [10], or by stirring the potential landscape [11].

In recent years a key development in condensate physics has been the creation of driven-dissipative Bose-Einstein condensates (BECs) of photons in microcavities filled with a fluorescent dye [12–14]. In contrast to conservative and polaritonic BECs, no superfluidity has so far been observed in photon condensates, because there is no significant photon-photon interaction [15,16]. Similar to thermalization, which is achieved through interaction with the dye molecules, coherence in the condensed light builds up only on account of the emission from the dye molecules [17]. While this mechanism is sufficient to result in the establishment of long-range phase coherence in a photon BEC [18–20], clear signatures of superfluidity such as the formation of vortices have remained elusive.

Our main goal is to theoretically explore to what extent a transient photon BEC can exhibit macroscopic coherence resembling that of a vortex. Rather than rotationally deforming the trapping potential, the dynamics in the condensate is driven by an orbiting pump spot. Stirring is thus achieved by

an incoherent and not a coherent mechanism. The resulting dynamical features share striking similarities with vortices in conservative BECs, which arise from superfluidity, but with some fundamental differences. For instance, the condensate forms a rigid spatial structure that rotates with the orbital frequency of the pump spot and has a high degree of phase coherence. However, in contrast to vortices in conservative condensates that have a density with continuous rotational symmetry, the photon BEC adopts a finely structured density with only a discrete rotational symmetry and an order that is determined by the orbital frequency of the pump spot.

In a typical setup, the photon gas inside the microcavity is restricted to a single longitudinal mode, denoted by the cavity cutoff frequency ω_0, while the mirror curvature imposes a harmonic potential on the two-dimensional (2D) transverse plane. The energy and wave function of the transverse cavity mode k is given by ω_k and $\psi_k(\mathbf{r})$. Now, an incoherent external pump with rate $\Gamma_\uparrow$ and focused on a fixed region or spot on the transverse plane produces a nonequilibrium distribution of excited dye molecules. The subsequent behavior of the emitted photons is dependent on the system properties, such as rate of absorption $\mathcal{A}_k$ and emission $\mathcal{E}_k$, and photon loss rate κ, as illustrated in Fig. 1(a). Importantly, the thermalization of photons is directly related to the total number of absorptions per unit photon loss, while the condensation transition is controlled by the pump rate. For an off-center pump, a transient photon wave packet is formed close to the pump spot [see Fig. 1(b)]. Under conditions for good thermalization, the photon wave packet collapses to the center to form a near-equilibrium Bose-Einstein condensate, whereas for poor thermalization, the stimulated light oscillates inside the harmonic trap imposed by the cavity mirrors. The formation and kinetics of a nonequilibrium, mode-locked photon wave packet in an effective one-dimensional space has been experimentally demonstrated using a pulsed pump [21]. Such transient behavior of light inside the cavity can be closely simulated using a microscopic, nonequilibrium model of photon condensation [22,23], which provides us the necessary theoretical tools for the study.
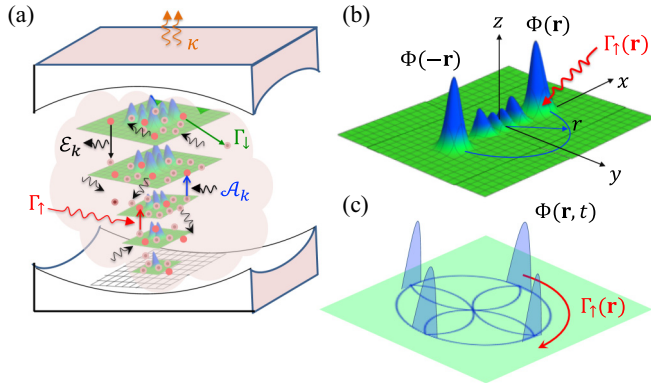
*himadri.dhar@iitb.ac.in

FIG. 1. (a) An illustration of a dye-filled microcavity, showing the first few nondegenerate cavity mode intensities, $|\psi_k(\mathbf{r})|^2$, on the 2D transverse plane. The absorption and emission rates for cavity mode k are given by $\mathcal{A}_k$ and $\mathcal{E}_k$, and κ is the rate of photon loss. $\Gamma_\uparrow$ is the pump rate and $\Gamma_\downarrow$ is the rate at which molecular excitation is lost to noncavity modes. (b) The spatially resolved photon wave packet, $\Phi(\mathbf{r})$, oscillating on the transverse xy plane, across the vertical cavity axis z, for an external pump focused at $\mathbf{r}$. (c) A qualitative picture of peaks forming during the time evolution of $\Phi(\mathbf{r}, t)$ due to periodic coming together of the oscillating wave packet in the harmonic trap and the orbiting pump.

Formation of structures. Photon emission with more enriched spatial features begin to appear in the transient dynamics when the focused pump spot is no longer static but orbiting in the transverse plane, as shown in Fig. 1(c). The dye molecules located within an annulus of radius r and width w determined by the orbit and width of the pump spot are initially excited. The optical modes that overlap with the annular region compete for these excitations and interfere to produce an initial displaced packet of light through stimulated emission (a nonequilibrium condensate). The evolution of the emitted photons is also dependent on the thermalization condition. Specifically, the low thermalization regime (absorption is slow compared to other processes), where nonequilibrium effects dominate, is favorable for the formation of spatial structures that exhibit phase coherence.

Shortly after the start of illumination, the photons begin to form a ring-shaped structure, which underlines the stimulated emission along the annular region traversed by the pump. This structure subsequently deforms and more complex spatial structures in the photon density begin to emerge. If the orbital frequency ν of the pump spot is a fraction of the frequency ω_T of the harmonic potential that traps the photon gas, i.e., $\nu = \omega_T/z$, where z is a positive integer, the photon density evolves towards a polygon pattern with a discrete rotational symmetry. Depending on whether z is odd or even, the polygon has z or $2z$ vertices, respectively, and the structure rotates with the orbital frequency ν of the pump spot. As the system evolves, the edges of the polygon disappear and a rigid structure with discrete peaks at the vertices is formed, with interference between the peaks. Such spatial structures, for both odd and even values of z, are shown in Fig. 2 in terms of the photon density $I(\mathbf{r}, t) = \sum_{k,k'} \Psi_{k,k'}(\mathbf{r}) n_{k,k'}(t)$ on the transverse plane of the cavity. Here $\Psi_{k,k'}(\mathbf{r}) = \psi_k^*(\mathbf{r})\psi_{k'}(\mathbf{r})$ and $n_{k,k'} = \langle \hat{a}_k^\dagger \hat{a}_{k'} \rangle$ are the mode overlap function and the
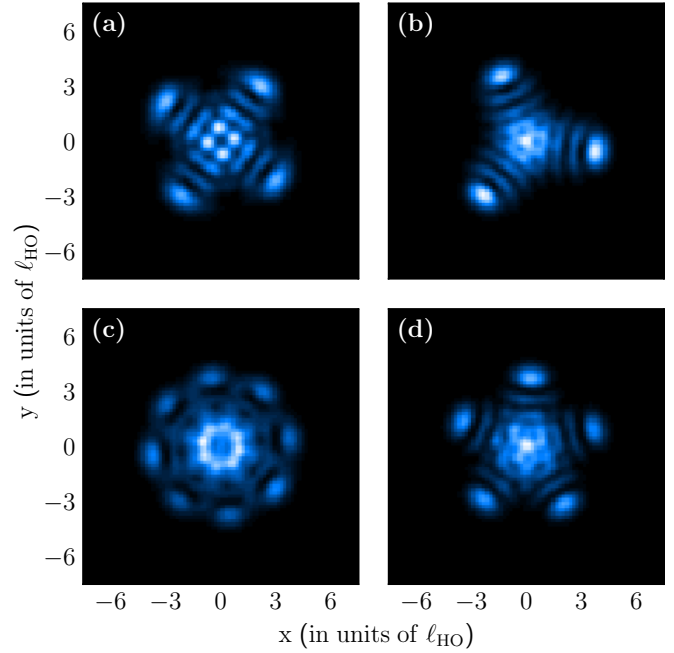

FIG. 2. Photon density $I(\mathbf{r})$ in the transverse plane of the cavity. The figure exhibits a snapshot of the photon emission when the dye-filled cavity is driven by an incoherent pump, focused at distance r away from the cavity center and circulating around this center with frequency $\nu = \omega_T/z$, where (a) $z = 2$, (b) $z = 3$, (c) $z = 4$, and (d) $z = 5$. All the axes are in units of harmonic oscillator length, ℓ_{HO}.

photon correlation, respectively. Once the spatial structure is formed it is robust and long-lived and becomes a characteristic feature of the condensate. For instance, for $\nu = \omega_T/2$, the intensity of the peaks and symmetric structure are visible even after more than 100 orbital periods have passed since the formation of the condensate. Further snapshots of the photon density at various moments during the evolution are given in the Supplemental Material [24].

The formation of the polygon structure and the discrete peaks can be qualitatively explained in terms of the motion of the photon wave packet arising from oscillations inside the harmonic trap and the motion of the focused pump spot. Once a wave packet is created as result of the pump, it will start oscillating in the trapping potential with a maximal displacement given by the radius r of the pump orbit. Due to dissipation, any such wave packet can persist only if it encounters the pump spot regularly, and the condition for this to happen is understood more easily by following the system dynamics in the frame corotating with the pump. In this frame, a wave packet follows curved trajectories as depicted in Fig. 1(c), and regular encounters with the pump spot are possible only if this curved trajectory forms a periodic orbit. The angle of rotation of the trajectory between instances of maximal displacement is given by $\pi(1 - 1/z)$, comprised of a contribution of π of the wave packet in the lab frame and a contribution of π/z of the pump. Thus the angular rotation of the wave packet after z instances of maximal displacement is given by $\pi(z - 1)$, which, in the case of odd z, is an integer multiple of 2π. In this case, the rosetta-shaped orbit of the wave packet is closed [as sketched in Fig. 1(c)], and it
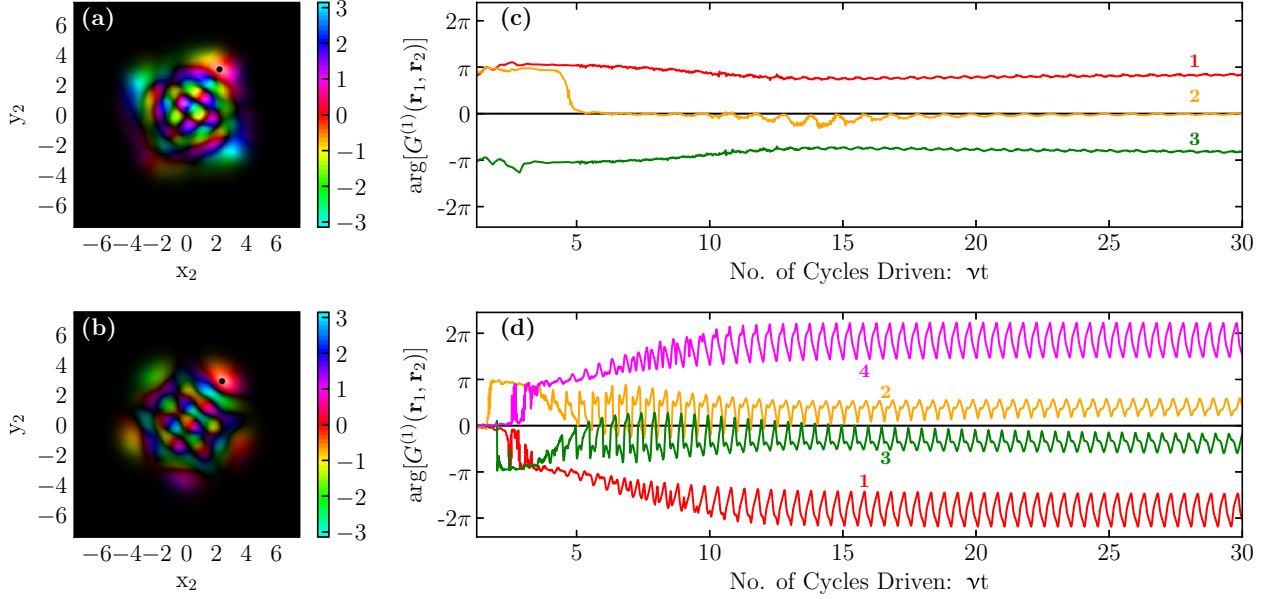
FIG. 3. First-order correlation function and phase relation in the condensed light. Subfigures (a) and (b) show $G^{(1)}(\mathbf{r}_1, \mathbf{r}_2)$ between a reference point $\mathbf{r}_1$ (shown by a dark dot) and any other spatial point $\mathbf{r}_2$, corresponding to orbital pump frequency $\nu = \omega_T/2$ [inset (a)] and $\nu = \omega_T/5$ [inset (b)] in the corotating frame. The color intensity (dark to bright) indicates the modulus of $G^{(1)}$, while the phase relation given by the argument is described by the color variation (color bar). Subfigures (c) and (d) show the unwrapped phase difference between the reference peak at $\mathbf{r}_1$ and the neighboring peaks numbered clockwise as 1–3 [in inset (c)] for structures with fourfold symmetry and numbered 1–4 [in inset (d)] for those with fivefold symmetry. An offset of -2π and 2π is added to peaks 1 and 4, respectively, for ease of viewing. All the axes in (a) and (b) are in units of harmonic oscillator length ℓ_{HO}, whereas for (c) and (d) the x axis is the scaled time νt and the y axis is in radians.

contains z points of maximal displacement, resulting in a z-fold symmetry. In the case of even z, on the other hand, it takes $2z$ instances of maximal displacement before the orbit closes and its symmetry is $2z$-fold. As such the complex structures result from the interplay between the nonequilibrium and driving mechanisms acting upon the photon gas.

Equations of motion. The transient photon density is numerically estimated from a set of nonlinear rate equations that not only describe the dynamics of the photons and the molecules (see Ref. [24] for details) but also provide a more quantitative approach to understand the spatial structures. The equation of motion for the photon correlation matrix $\mathbf{n}$ with elements $n_{k,k'} = \langle \hat{a}_k^\dagger \hat{a}_{k'} \rangle$ is given by

$$\dot{\mathbf{n}} = \left(i\mathbf{\Omega} - \frac{\kappa}{2} \right) \mathbf{n} + \rho_0 \{ \mathbf{f} \, \mathbf{E}(\mathbf{n} + \mathbb{I}) + (\mathbf{f} - \mathbb{I})\mathbf{A}^\dagger \mathbf{n} \} + \text{H.c.,} \tag{1}$$

where $\mathbf{f}$ is the molecular excitation matrix with elements $f_{k,k'} = \sum_i \Psi_{k,k'}(\mathbf{r}_i) \langle \sigma_i^+ \sigma_i^- \rangle$ and ρ_0 is the molecular density. The absorption and emission matrices are given by $E_{k,k'} = \mathcal{E}_k \delta_{k,k'}$ and $A_{k,k'} = \mathcal{A}_k \delta_{k,k'}$, respectively. Moreover, $\Omega_{k,k'} = \omega_k \delta_{k,k'}$, where ω_k is the energy of the cavity mode k and $\mathbb{I}$ is the identity matrix. The equation of motion for the molecular excitation vector $\mathbf{m}$, with elements $m_j = \sum_i \delta(\mathbf{r}_j - \mathbf{r}_i) \langle \sigma_i^+ \sigma_i^- \rangle$, is given by

$$\dot{\mathbf{m}} = -\{ \Gamma_\downarrow + 2\mathbf{E}_{\text{eff}} \} \mathbf{m} + \{ \Gamma_\uparrow(\mathbf{r}) + 2\mathbf{A}_{\text{eff}} \}(\mathbf{1} - \mathbf{m}), \tag{2}$$

where $\mathbf{E}_{\text{eff}} = \text{Tr}[\psi(\mathbf{r})\mathbf{E}(\mathbf{n} + \mathbb{I})]$ and $\mathbf{A}_{\text{eff}} = \text{Tr}[\psi(\mathbf{r})\mathbf{n}\mathbf{A}]$.

Analytical model. The motion of the photon wave packet and the formation of the condensate can be explained in terms of the nonequilibrium dynamics of the system. A sim-

plified picture can be constructed by rewriting Eq. (1), as $\dot{\mathbf{n}} = \mathcal{F}^{(0)} + i\mathcal{F}^{(1)}$, where $\mathcal{F}^{(0)}$ is the nonoscillatory component and $\mathcal{F}^{(1)}$ oscillates with $\Omega_{k,k'}$. In the absence of $\mathcal{F}^{(1)}$, the rate equation for the photon correlation is $\dot{n}_{k,k'} = \mathcal{F}^{(0)}_{k,k'}$. For a constant pump at $\mathbf{r}$ and after a long time τ, the photons condense to form a localized wave packet $\Phi(\mathbf{r}, \tau)$, which is the steady state, i.e., $\bar{n}_{k,k'}(\tau) = \text{Tr}[\hat{a}_k^\dagger \hat{a}_{k'} \Phi(\mathbf{r}, \tau)]$ is the steady solution for $\dot{\bar{n}}_{k,k'} = \mathcal{F}^{(0)} = 0$. To approximate the oscillatory dynamics, the term $\mathcal{F}^{(1)}$ is introduced at $t > \tau$ to obtain a new equation of motion $\dot{n}_{k,k'} = i(\omega_k - \omega_{k'})\bar{n}_{k,k'}$, with solution $\bar{n}_{k,k'}(t) = \bar{n}_{k,k'}(\tau) \exp[i\Delta\omega_{k,k'} t]$. Here $\Delta\omega_{k,k'} = \omega_k - \omega_{k'}$ is the gap between neighboring energy modes of the cavity. The photon density is then given by $I(\mathbf{r}) = \sum_{k,k'} \Psi_{k,k'} \bar{n}_{k,k'}(\tau) \exp[i\Delta\omega_{k,k'} t]$.

Now, for 2D harmonic oscillators, the frequency of mode k is given by $\omega_k = \omega_0 + (q_x + q_y)\omega_T$, corresponding to the quantum numbers $\{q_x, q_y\}$ and the cutoff frequency ω_0. Since the pump spot is focused at r, the condensed light is mostly found in the annular domain of radius r. The highly populated modes thus have a maximum amplitude around this domain. These modes are characterized by the condition $q_x + q_y = q, q \pm 1$, where q is the integer closest to $r^2/(2\ell_{HO}^2)$, and ℓ_{HO} is the harmonic oscillator length [24]. Since degenerate modes do not contribute to the oscillation, as $\Delta\omega_{k,k'} = 0$, the oscillation comes from nondegenerate modes with q and $q \pm 1$, for which $\Psi_{k,k'}(\mathbf{r}) = \psi_k^*(\mathbf{r})\psi_{k'}(\mathbf{r})$ is an odd function. At $t = n\pi/\omega_T$, the density is given by $I(\mathbf{r}) = \sum_{k,k'} \Psi_{k,k\pm1}(\mathbf{r})\bar{n}_{k,k\pm1}$, for even n, and by $I(-\mathbf{r}) = -\sum_{k,k'} \Psi_{k,k\pm1}(\mathbf{r})\bar{n}_{k,k\pm1}$, for odd n. Therefore the wave packet $\Phi(\mathbf{r}, \tau)$ oscillates between the positions $\mathbf{r}$ and $-\mathbf{r}$ in the cavity plane with frequency ω_T. The

transient spatial structure then arises due to the interference between the wave functions of the dominant modes with q and $q \pm 1$.

The discrete rotational symmetry with the odd-even dichotomy, as discussed earlier, results from $\Phi(\mathbf{r}, \tau)$ being influenced by the two competing frequencies, viz. the harmonic trap frequency ω_T and the pump orbital frequency ν. The constructive interference or beats occur with frequency $\frac{1}{2}(\omega_T - \nu)$ and yields a factor of $\frac{1}{2}(1 - 1/z)$ in the angular rotation, which ultimately gives rise to the z- or $2z$-fold angular symmetry, as discussed earlier. The discrete symmetry is robust to deviations of z from integer values, but for ostensibly noncommensurate values of the frequencies, the light is spread along the annular region surrounding the pump orbit with no clear spatial structure [25].

Phase coherence. The transient structures of the photon density depicted in Fig. 2 are consistent with phase coherence in the system, and the explanations given so far are based on the assumption of at least partially coherent dynamics. However, unambiguous evidence of phase coherence, cannot be obtained from density profiles alone. A proper verification of phase coherence needs to be obtained in terms of the first-order correlation between photons at different points in the cavity plane. By introducing the field operators $\hat{\xi}(\mathbf{r}) = \sum_k \psi_k(\mathbf{r}) \hat{a}_k$ and its conjugate $\hat{\xi}^\dagger(\mathbf{r}) = \sum_k \psi_k^*(\mathbf{r}) \hat{a}_k^\dagger$, the first-order correlation function is defined as $G^{(1)}(\mathbf{r}_1, \mathbf{r}_2, t) = \langle \hat{\xi}^\dagger(\mathbf{r}_1) \hat{\xi}(\mathbf{r}_2) \rangle = \sum_{k,k'} \psi_k^*(\mathbf{r}_1) \psi_{k'}(\mathbf{r}_2) n_{k,k'}(t)$. Figures 3(a) and 3(b) show the correlation function $G^{(1)}(\mathbf{r}_1, \mathbf{r}_2)$ in the corotating frame between a fixed reference point $\mathbf{r}_1$ (shown by a dark dot) and any other point $\mathbf{r}_2$ in the transverse plane. The figures correspond to the orbital pump frequencies $\nu = \omega_T/z$ for $z = 2$ in inset (a) and $z = 5$ in inset (b). The color intensity (dark to bright) denotes the modulus of $G^{(1)}(\mathbf{r}_1, \mathbf{r}_2)$, which exhibits either a four- or fivefold rotational symmetry, consistent with the photon density of the condensed light for odd and even z. The color map highlights the argument of $G^{(1)}(\mathbf{r}_1, \mathbf{r}_2)$, which gives us the phase resulting from the interference between the modes. Despite the detailed structure of the photon density with several minima (in black), one can see a clear closed phase evolution for radii of about $3l_{HO}$ winding around the center. Similar vortexlike phase windings are also observed on a smaller scale.

The phase has a fixed relation in the corotating frame, as seen in Figs. 3(c)–3(d), where the phase difference between the spatial points corresponding to the different photon density peaks is depicted as a function of time. For $z = 2$ there are four peaks (numbered 0–3, clockwise), and in the ideal case it is expected that the phase difference between a reference peak 0 at $\mathbf{r}_1$ and its neighboring peaks 1 and 3 is $\pm\pi$, while it is in phase (2π) with the diametrically opposite peak 2. This is because for $z = 2$, the beat phenomenon results in all the peaks being formed in a single pump cycle. Figure 3(c) shows that the phase correlations converge to these values with time. The situation is more complicated for $z = 5$, where the five peaks (numbered 0–4, clockwise) are formed over two pump cycles. Hence, taking a reference peak 0 at $\mathbf{r}_1$, the phase difference with the neighboring peak 1 and 4 changes between $\mp\pi/5$ and $\pm3\pi/5$, respectively, and for the distant peaks 2 and 3 between $\pm\pi/5$ and $\pm3\pi/5$, respectively, as seen in Fig. 3(d).

Discussion and outlook. Experimental realization of the spatial structures identified here requires an orbiting pump spot in an otherwise standard room-temperature photon BEC experiment [26]. Since this can be implemented by interfering two Laguerre-Gaussian beams of different order and frequency, experimental observation of these structures would provide very compelling evidence of well-defined coherence properties that can be established despite the absence of any effective particle interaction. The present results thus not only indicate a pathway towards the observation of vortexlike phenomena in photon BECs, but they also support the expectation that features like superfluidity that are common in atomic and quasiparticle BECs can also be extended to photons if suitable driving mechanisms are identified.

While the present analysis applies to a regime of large photon numbers, the interference mechanisms resulting in the formation of coherent spatial structures exist for light of any level of intensity, right down to the few-photon regime. Since the photon number in a BEC can be controlled in terms of mirror curvature [27,28], the ability to create well-designed states of light through temporally tuned driving is thus applicable to a broad range of regimes. Given the notorious difficulty in preparing nonclassical few-photon states of light and their potential for quantum-technological applications, the present work thus may inspire an unconventional handle on the control of quantum states of light.

---

[1] G. Falkovich, *Fluid Mechanics*, 2nd ed. (Cambridge University Press, Cambridge, 2018).

[2] A. Wachowiak, J. Wiebe, M. Bode, O. Pietzsch, M. Morgenstern, and R. Wiesendanger, Direct observation of internal spin structure of magnetic vortex cores, Science **298**, 577 (2002).

[3] G. Blatter, M. V. Feigel'man, V. B. Geshkenbein, A. I. Larkin, and V. M. Vinokur, Vortices in high-temperature superconductors, Rev. Mod. Phys. **66**, 1125 (1994).

[4] W. Ketterle, Nobel lecture, When atoms behave as waves: Bose-Einstein condensation and the atom laser, Rev. Mod. Phys. **74**, 1131 (2002).

[5] A. J. Leggett, Superfluidity, Rev. Mod. Phys. **71**, S318 (1999).

[6] I. Carusotto and C. Ciuti, Quantum fluids of light, Rev. Mod. Phys. **85**, 299 (2013).

[7] K. G. Lagoudakis, M. Wouters, M. Richard, A. Baas, I. Carusotto, R. André, Le Si Dang, and B. Deveaud-Plédran,

Quantized vortices in an exciton-polariton condensate, Nat. Phys. **4**, 706 (2008).

[8] A. Amo, J. Lefrére, S. Pigeon, C. Adrados, C. Ciuti, I. Carusotto, R. Houdré, E. Giacobino, and A. Bramati, Superfluidity of polaritons in semiconductor microcavities, Nat. Phys. **5**, 805 (2009).

[9] J. Kasprzak, M. Richard, S. Kundermann, A. Baas, P. Jeambrun, J. M. J. Keeling, F. M. Marchetti, M. H. Szymańska, R. André, J. L. Staehli, V. Savona, P. B. Littlewood, B. Deveaud, and Le Si Dang, Bose-Einstein condensation of exciton polaritons, Nature (London) **443**, 409 (2006).

[10] J. D. Rodrigues, J. T. Mendonça, and H. Terças, Turbulence excitation in counterstreaming paraxial superfluids of light, Phys. Rev. A **101**, 043810 (2020).

[11] J. R. Abo-Shaeer, C. Raman, J. M. Vogels, and W. Ketterle, Observation of vortex lattices in Bose-Einstein condensates, Science **292**, 476 (2001).

[12] J. Klaers, J. Schmitt, F. Vewinger, and M. Weitz, Bose-Einstein condensation of photons in an optical microcavity, Nature (London) **468**, 545 (2010).

[13] J. Marelic and R. A. Nyman, Experimental evidence for inhomogeneous pumping and energy-dependent effects in photon Bose-Einstein condensation, Phys. Rev. A **91**, 033813 (2015).

[14] S. Greveling, K. L. Perrier, and D. van Oosten, Density distribution of a Bose-Einstein condensate of photons in a dye-filled microcavity, Phys. Rev. A **98**, 013810 (2018).

[15] H. Alaeian, M. Schedensack, C. Bartels, D. Peterseim, and M. Weitz, Thermo-optical interactions in a dye-microcavity photon Bose-Einstein condensate, New J. Phys. **19**, 115009 (2017).

[16] R. A. Nyman and M. H. Szymańska, Interactions in dye-microcavity photon condensates and the prospects for their observation, Phys. Rev. A **89**, 033844 (2014).

[17] D. W. Snoke and S. M. Girvin, Dynamics of phase coherence onset in Bose condensates of photons by incoherent phonon emission, J. Low Temp. Phys. **171**, 1 (2013).

[18] J. Schmitt, T. Damm, D. Dung, C. Wahl, F. Vewinger, J. Klaers, and M. Weitz, Spontaneous Symmetry Breaking and Phase Coherence of a Photon Bose-Einstein Condensate Coupled to a Reservoir, Phys. Rev. Lett. **116**, 033604 (2016).

[19] J. Marelic, L. F. Zajiczek, H. J. Hesten, K. H. Leung, E. Y. X. Ong, F. Mintert, and R. A. Nyman, Spatiotemporal coherence of non-equilibrium multimode photon condensates, New J. Phys. **18**, 103012 (2016).

[20] T. Damm, D. Dung, F. Vewinger, M. Weitz, and J. Schmitt, First-order spatial coherence measurements in a thermalized two-dimensional photonic quantum gas, Nat. Commun. **8**, 158 (2017).

[21] J. Schmitt, T. Damm, D. Dung, F. Vewinger, J. Klaers, and M. Weitz, Thermalization kinetics of light: From laser dynamics to equilibrium condensation of photons, Phys. Rev. A **92**, 011602(R) (2015).

[22] P. Kirton and J. Keeling, Nonequilibrium Model of Photon Condensation, Phys. Rev. Lett. **111**, 100404 (2013).

[23] J. Keeling and P. Kirton, Spatial dynamics, thermalization, and gain clamping in a photon condensate, Phys. Rev. A **93**, 013829 (2016).

[24] See Supplemental Material at http://link.aps.org/supplemental/10.1103/PhysRevA.104.L031505 for extended discussion on the nonequilibrium model of photon condensation, additional figures on the dynamics of the photon gas and formation of spatial structures, and the occupation of relevant modes that produce the interference patterns.

[25] For z that are not integers, there is a qualitative tradeoff between the amount by which z is noncommensurate and the time over which spatial structures are robust. For z close to an integer, the spatial structures remain distinctly visible over a substantially longer period, in contrast to the opposite case where the discrete structure becomes unclear relatively early.

[26] J. Klaers, F. Vewinger, and M. Weitz, Thermalization of a two-dimensional photonic gas in a 'white wall' photon box, Nat. Phys. **6**, 512 (2010).

[27] B. T. Walker, L. C. Flatten, H. J. Hesten, F. Mintert, D. Hunger, A. A. P. Trichet, J. M. Smith, and R. A. Nyman, Driven-dissipative non-equilibrium Bose-Einstein condensation of less than ten photons, Nat. Phys. **14**, 1173 (2018).

[28] J. D. Rodrigues, H. S. Dhar, B. T. Walker, J. M. Smith, R. F. Oulton, F. Mintert, and R. A. Nyman, Learning the Fuzzy Phases of Small Photonic Condensates, Phys. Rev. Lett. **126**, 150602 (2021).